DOI: 10.37190/ABB-02481-2024-03

Influence of sterilization and exposure to the Ringer's solution on physicochemical properties of nitrocarburized 316 LVM steel

Anita Kajzer[1*], Klaudiusz Gołombek[2], Bogusław Ziębowicz[2], Tomasz Borowski[3]

[1] Faculty of Biomaterials and Medical Devices Engineering, Faculty of Biomedical Engineering, Silesian University of Technology, Zabrze, Poland

[2] Faculty of Engineering Materials and Biomaterials, Silesian University of Technology, Gliwice, Poland

[3] Faculty of Materials Science and Engineering, Warsaw University of Technology, Warsaw, Poland

[*]Corresponding author: Anita Kajzer, Faculty of Biomaterials and Medical Devices Engineering, Faculty of Biomedical Engineering, Silesian University of Technology, Zabrze, Poland, e-mail address: Anita.Kajzer@polsl.pl

Submitted: 16th July 2024

Accepted: 20th September 2024

Abstract

Purpose The aim of the study was to investigate the influence of the nitrocarburizing process carried out in low temperature plasma using the active screen at 440°C on the structure and physicochemical properties of the 316LVM steel. *Methods* In the paper results of microstructure and phase composition of the layers, roughness, and surface wettability, potentiodynamic pitting corrosion resistance, penetration of ions into the solution as well as biological tests were present. The studies were conducted for the samples of both mechanically polished and nitrocarburized surfaces, after sterilization, and exposure to the Ringer's solution. *Results* Based on the obtained results the influence of sterilization and exposure to Ringer's solution on the physicochemical properties of the surface of both the substrate and the layer were determined. The formation of a nitrocarburizing layer resulted in a favorable increase in the tested parameters were observed. *Conclusions* In the conclusion, the suitability of the proposed 316LVM steel surface treatment method for short-term implants can be confirmed.

Key words: 316LVM steel, nitrocarburization, corrosion resistance, surface wettability, biocompatybility

1. Introduction

The treatment of anterior chest wall defects using the Nuss method involves the use of multi-element metal stabilizers made of 316LVM steel or titanium alloys. Their use may be associated with adverse events that affect the patient's condition. However, due to the very good stabilization effect, low minimally invasiveness, less postoperative pain and very good cosmetic effect, this method is very often used by thoracic surgeons around the world [7,21,36,38]. Stabilization of a deformed chest using the Nuss method is most often performed in patients aged 17-21, however, due to it’s minimally invasiveness, it is also used in children under 10 years of age – Fig. 1.

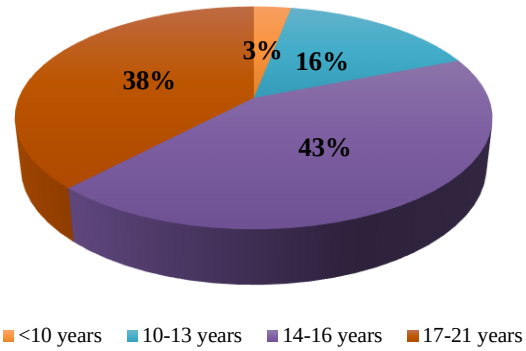

Fig. 1. Age of patients treated with the Nuss method [7]

According to literature [11], from 0.5% to 2.5% of planned procedures are associated with the occurrence of intraoperative adverse events. A progressive adverse event in the form of infection in the area of the implant may cause histopathological changes in the bone at the site of contact with the implant, most often through the development of inflammatory granulation tissue [27,29,34]. Such consequences were described by the authors [12], who performed 862 stabilizations using the Nuss method over an 18-year period (1987-2005). Nineteen patients (2.2%) aged 9 to 23 were diagnosed with an allergy to the components of the metal implant. In particular, in this group, 63% of patients developed rash and erythema, 6% had inflammatory granulation tissue, and 31% had pleural effusion (Fig. 2). In these cases, the 316LVM steel plate had to be removed from the body, while in three patients it was replaced with a titanium plate.

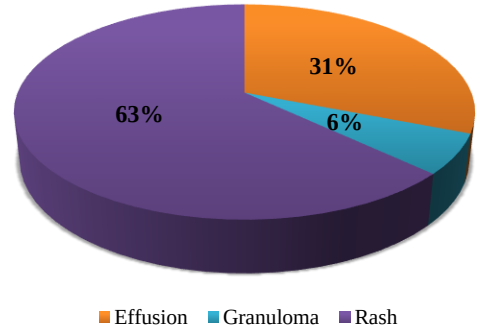

Fig. 2. Symptoms of allergy after insertion into the chest plate made of 316LVM steel [12]

In multi-element stabilizers, displacements occur during anatomical loading. This leads to the formation of friction pairs that damage the passive layer of the implant surface. These conditions, combined with the aggressive impact of the tissue environment, favor the development of corrosion [18,23,37]. Corrosion products: i.e. ions of alloying elements from

the implant released into the tissue environment and body fluids, participate in synergistic or antagonistic reactions. The observed histopathological reactions in the tissues depend mainly on the type of biomaterial. For example, nickel allergy can cause a complex inflammatory condition similar to sepsis. This is manifested by: local skin inflammation, edema, lymphadenopathy [1], recurrent infections [30] and poor wound healing [31]. Increased exposure to nickel stimulates and duplicates "T" cells, which, if they reach the so-called tolerance test, cause the occurrence of the above symptoms [32]. Therefore, it is so important to increase the biocompatibility of implants. Increase of the corrosion resistance, and surface hardness as well, can be obtained by surface treatment [3,6,20,26,39,38]. More and more often processes of plasma or gas nitriding, or ion implantation are used [2,5,24]. Recently also the process of glow discharge nitrocarburizations is used. The mentioned technology combines the process of low-temperature nitriding and carburization in a low-temperature plasma, in which, next to a mixture of nitrogen and hydrogen, a methane is used [8,19]. This process enables the production on the austenitic stainless steel a double layer of nitrogen austenite γ_N and carbon austenite γ_C. Application of the modified process realized with the use of the active screen allows to process complex shape parts [9,33], which is especially important for medical instruments and implants. This technology allows for keeping a certain surface roughness, due to the reduction of the sputtering effect, resulting in improved mechanical and corrosion properties of these layers. A comprehensive solution to improve the quality of 316LVM steel used in orthopedic implants should be focused on shaping the structure of the diffusion surface layer including the sterilization process and tissue environment.

The need for such studies is required in various fields. However, in biomedical engineering from cardiology, through dentistry and orthopedics, they are special and regulated by dedicated normative regulations. The results of these studies are addressed to companies operating in the field of medical device production.

Therefore, the aim of the study was to investigate the influence of the nitrocarburizing process carried out in low temperature plasma using the active screen at 440°C on the structure and properties of the 316LVM steel.

2. Material and methods

The studies were conducted on stabilizers for the treatment of anterior chest wall deformities made of 316 LVM steel with chemical composition and mechanical properties consistent with the recommendations of ISO 5832-1:2020 [16]. Based on the results of

microscopic metallographic examinations, non-metallic inclusions in the form of globular oxides were found in the steel structure - Fig. 3a. In the steel structure, elongated austenite grains with numerous slip bands were distinguished - Fig. 3b, c. The tested material met the recommendations included in the subject standard ISO 5832-1, which was verified during preliminary tests.

a) b) c)

Fig. 3. Non-metallic inclusions in the form of globular oxides – a), austenitic structure with slip bands – transverse b), longitudinal – c), light microscope

The surface modification of the stabilizers was carried out by: grinding, electrochemical polishing, passivation. The prepared samples were subjected to the glow discharge plasma assisted nitrocarburizing using the active screen made of the Fe-Cr-Ni [5]. The nitrocarburizing process was carried out at 420°C. The pressure in the working chamber was equal to 2 hPa. The composition of the working mixture was as follows: N_2, H_2, and CH_4 47:143:10, time of proces t=2h. The surfaces prepared in this way were subjected to medical sterilization and exposure to Ringer's solution simulating the tissue environment. The samples were kept for 28 days at 37 °C in the laboratory incubator 53 FD (BINDER). Additionally, sterilization with ethylene oxide was performed before biological tests. The samples were then divided into the 6 groups acording to table 1.

Table 1. Samples for testing

Electrochemically polished	
PE	Electrochemically polished and chemically passivated
PES	Electrochemically polished and chemically passivated after sterilization
PESR	Electrochemically polished and chemically passivated after sterilization and exposure to Ringer's solution
Nnitrocarburizing layer (γ_{NC})	
ANC	Nnitrocarburizing layer (γ_{NC})
ANCS	Nnitrocarburizing layer (γ_{NC}) after sterilisation
ANCSR	Nnitrocarburizing layer (γ_{NC}) after sterilization and exposure to Ringer's solution

2.1. Chemical composition and microstructure of the layer

The evaluation of the stabilizer microstructure was carried out on the cross-section using transmission electron microscopy (TEM) techniques. The THEMIS FEG microscope from ThermoFisher was used for the analyses. The thin film was prepared using the focused gallium ion beam technique on the DualBeam SCIOS II microscope from the ThermoFisher. First, the microstructure was assessed in the bright field observation (TEM BF). Phase analysis from selected locations was performed using electron diffraction (SAEDP) from the layer area and from the substrate area. Additionally, a qualitative analysis of the chemical composition was performed using EDS. The analysis results were presented in the form of maps of the distribution of elements such as: Fe, C and N.

2.2. Surface topography

Surface topography studies of all sample groups were conducted using a ZEISS Supra 25 scanning electron microscope and a Park Systems XE-100 atomic force microscope (AFM). The QBSD detector and an accelerating voltage of 20,000 kV were used for SEM analysis. The QBSD detector was used to assess the surface structure in the scanning electron microscope, while the SE detector was used to assess the topography of the deformed samples with a layer.

In AFM studies, the non-contact mode of the microscope was used, in which the tip was moved 1-10 nm away from the surface for imaging. The Sa parameter was calculated in the XEI program integrated with the AFM microscope, which is a tool for editing and processing the obtained images.

2.3. Surface wettability

To determine the wettability of the surface, contact angle and the surface free energy (SFE) measurements, by means of the Owens-Wendt method were used. Contact angle measurements with distilled water (θ_d) (Merck) and diiodomethane (θ_w) (Poch SA) were conducted using a drop of liquid with a volume of 1.5 ml. The measurements were performed by applying the SURFTENS UNIVERSAL optical goniometer (OEG) and the computer software Surftens 4.5 for analyzing the recorded image of the drops. The measurements were carried out at room temperature (T=23±1°C) for 60 seconds.

2.4. Potentiodynamic study

The study of pitting corrosion resistance was carried out by means of the potentiodynamic method using three electrodes: the reference electrode (saturated calomel electrode - Ag/AgCl

3M KCl), the auxiliary electrode (platinum electrode PtP-201), and the working electrode – the sample. The study was realized with the use of the VoltaLab PGP 201 potentiostat equipped with the Volta Master software. The study consisted in recording polarization curves in accordance with the recommendation of the PN-EN ISO 10993-15 standard [28]. On the basis of the obtained curves the following corrosion parameters were determined: corrosion potential E_{corr}. breakdown potential E_b, repassivation potential E_{cp}, transpassivation potential E_{tr} and, using the Stern method, polarization resistance R_p. The studies were performed in the Ringer's solution at the temperature of $T = 37\pm1°C$.

2.5. Ions infiltration

In order to assess coating density of the surface layer and also the amount of ions infiltrating from the steel to the Ringer's solution, metallic ions permeability tests were performed. The amount of Fe, Si, Cr, Ni and Mo ions that infiltrated to the solution was designated. Each sample was placed for 28 days in 100 ml of the Ringer's solution at the temperature of $T = 37\pm1°C$. Metallic ions concentrations were measured with the JY 2000 spectrometer (by Yobin – Yvon) applying the ICP-AES method.

2.6. Cytotoxicity studies

The cytotoxicity and cell viability tests were performed using the direct method (according to ISO 10993-5) [15] using human fibroblast cells (PromoCell, DE), which consisted in determining the probability and number of necrotic cells on the analyzed surfaces in relation to live cells (first method) and determining the amount of lactate dehydrogenase secreted from cells that had direct contact with the surface (second method). In the first method, two dyes were used - propidium iodide (PI) and MitoTracker Green FM (Mitochondrion-Selective Probes), a green fluorescent mitochondrial dye. Cell viability was assessed after a 24-hour incubation using a confocal scanning microscope (Exciter 5, Carl Zeiss). In the second method, after conducting cell culture on the surfaces of the tested materials, the supernatant was collected in a volume of 100 µl for measuring lactate dehydrogenase LDH. The LDH level was determined using a spectroscopic method (EPOCH2 spectrophotometer by BioTek) through changes in absorbance observed per unit of time, which is a measure of the reaction rate.

3. Results

3.1. Chemical composition and microstructure of the layer

For all layers (ANC, ANCS, ANSCR), point diffraction lines were found in the surface layer, indicating a coarse-grained structure (diffraction from a single grain). For the carbon-nitrogen layer, the $Fe_4(Fe(CN)_6)_3$ phase with a regular, flat-centered structure was identified – Fig. 4. Based on the obtained diffraction lines, austenitic steel was identified for the substrate and the presence of the Cr0.19Fe0.7Ni0.11 phase, also with a regular, flat-centered structure was found.

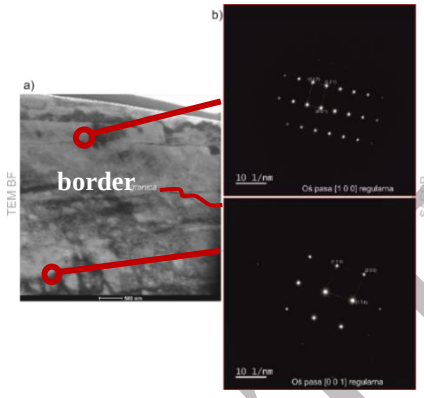

Fig. 4. Example microstructural analysis, for the layer after the initial state (ANC): a) image in the bright field of view (TEM BF), b) phase analysis by electron diffraction (SAEDP)

The results of the analysis (EDS) of the carbon-nitrogen layer in the form of distribution maps of selected elements for samples in the initial state are presented in Fig. 5b, 59b. In all cases, a gradient of N and C concentration was recorded, indicating a decrease in the share of C and N with the distance from the surface. Visible changes occurred to a depth of approx. 1.5 μm from the surface.

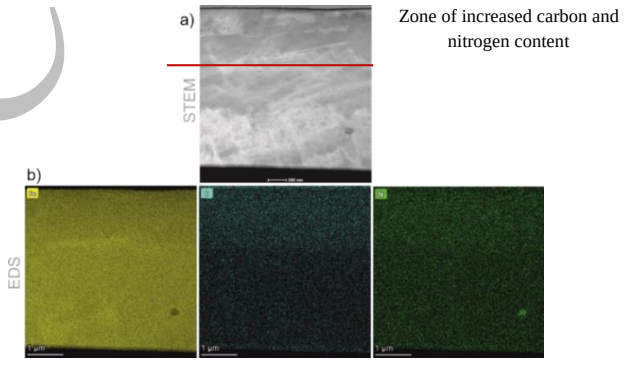

Fig. 5. Qualitative analysis of the chemical composition, EDS, for the layer in the initial state (ANC): a) STEM image from the analysis area, b) distribution maps, respectively: Fe, C, N

Additionally, for the layer after sterilization and exposure to Ringer's solution, a bulge was observed on the surface of the material, which was caused by local corrosion – Fig. 6a, which

was confirmed during the pitting corrosion resistance tests. The analysis of the chemical composition carried out for both the unchanged surface and the local corrosion sites confirmed the gradient content of carbon and nitrogen, which is consistent with the nitrocarburization process (Fig. 6b).

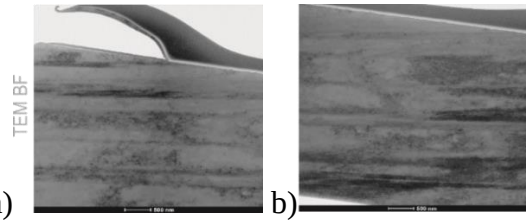

a) b)

Fig. 6. Example microstructure analysis, TEM, for a layer (ANCSR): a) image in the bright field of view (TEM BF): a) local corrosion, b) surface without corrosion changes

3.2. Surface topography

The results of the surface topography studies were presented in Figs. 7-9 and in Table 11. Based on SEM analysis, the surface of electrochemically polished samples revealed the presence of an austenitic structure with visible slip bands and annealing twins, indicating the performed plastic processing of the biomaterial – Fig. 7. On the other hand, the surface of samples with a layer showed carbon-nitrogen austenite – Fig. 8. No effect of sterilization and exposure to Ringer's solution on the surface morphology was found for both polished and layered samples. For samples with a layer after sterilization (ANCS) and exposure (ANCSR) subjected to bending by an angle of 80° on their external surface, at 1000x magnification, a larger number of microcracks were observed for ANCSR samples – Fig. 9.

Based on the AFM analysis, differences in the Sa parameter values were found – Figs. 10, 11 and Table 2. Both sterilization and exposure to Ringer's solution increased the surface roughness. Smaller differences were observed for the surface of the samples with a layer. The formation of the layer didn’t significantly affect the change in roughness in relation to the substrate. The largest difference in values occurs for the samples exposed to Ringer's solution.

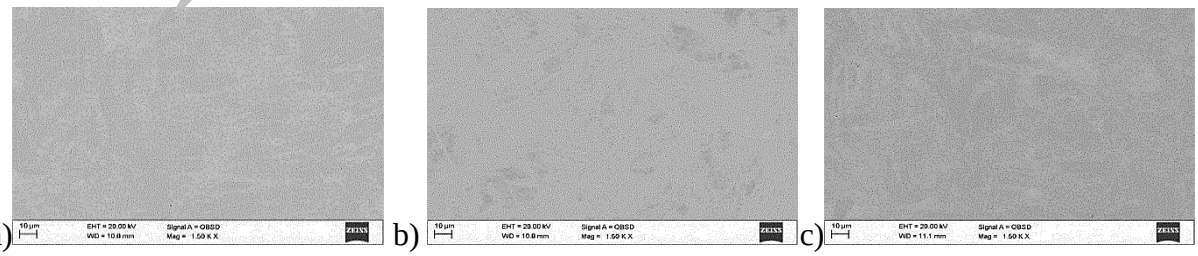

a) b) c)

Fig. 7. Example of surface topography of the polished samples, SEM: a) PE, b) PES, c) PESR

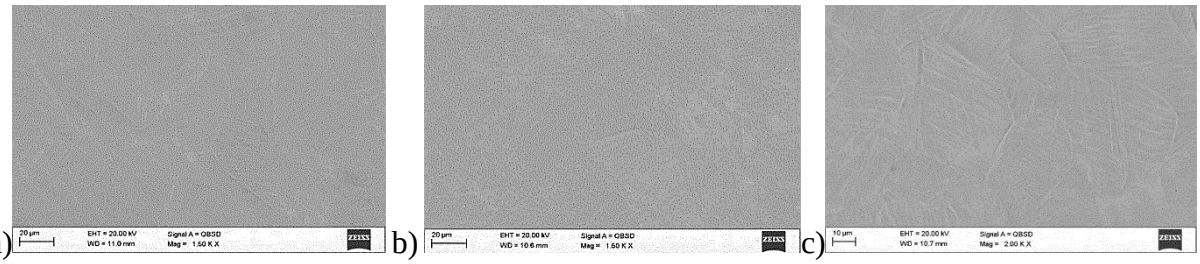

Fig. 8. Example of surface topography of the layer, SEM: a) ANC, b) ANCS, c) ANCSR

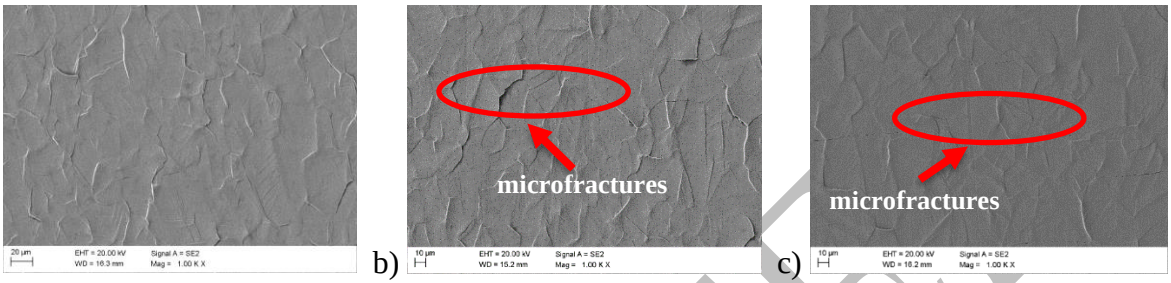

Fig. 9. Example of surface topography of the layer, after deformation: a) ANC, b) ANCS, c) ANCSR

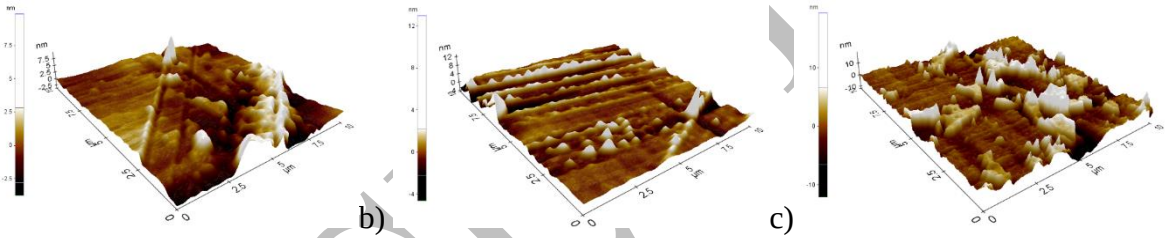

Fig. 10. Example morphology of the polished surface, AFM: **a**) PE, **b**) PES, **c**) PESR

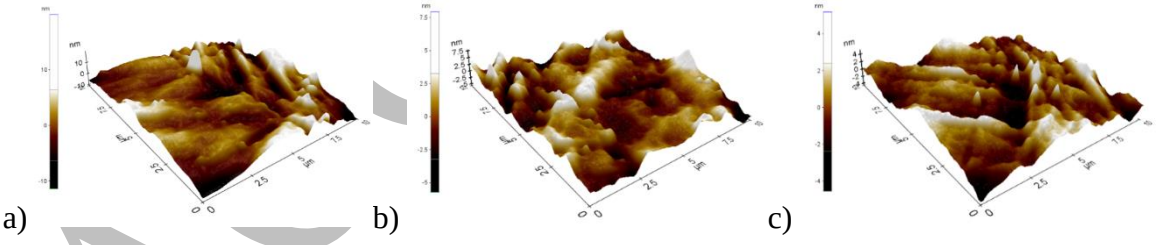

Fig. 11. Example morphology of the layer, AFM: **a**) ANC, **b**) ANCS, **c**) ANCSR

Table 2. Surface roughness test results

		PE	PES	PESR	ANC	ANCS	ANCSR
Sa, nm	**Av.**	**25**	**86**	**164**	**29**	**65**	**79**
	SD	5	12	14	9	12	11

3.3. Surface wettability

The results of the study were presented in Figs. 12 and 13 and in Table 3. The formation of a carbon-nitrogen layer caused an increase in the angle value in relation to the samples subjected to electrochemical polishing. The highest values of angles indicating hydrophobic properties in

this case for both PE and ACN samples were observed for the initial state. On the other hand, the sterilization and exposure processes caused a change in the surface character from hydrophobic to hydrophilic, but with low wettability. Taking into account the obtained standard deviations, it can be stated that for the PES and ANCS variants no significant differences were observed in the values of angles θ_{av}. A greater difference was observed for the PESR and ANCSR variants, while for ANCSR the wettability was lower.

No significant differences were found in the surface free energy (SFE) values for the coated surface compared to the polished samples.

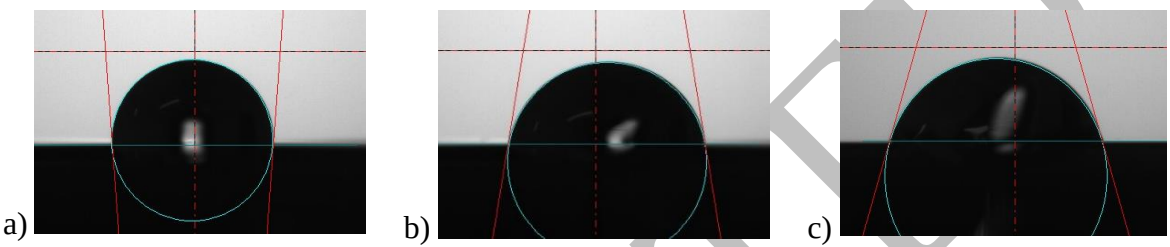

Fig. 12. Examples of a drop during measurement: a) PE ($\theta_{śr}$ = 90.7°), b) PES ($\theta_{śr}$ = 78.3°), c) PESR ($\theta_{śr}$ = 73.2°)

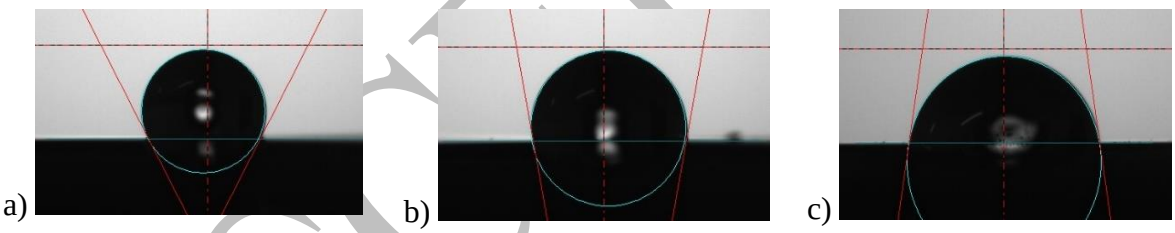

Fig. 13. Examples of a drop during measurement: a) ANC ($\theta_{śr}$ = 113.5°). b) ANCS ($\theta_{śr}$ = 94.3°), c) ANCSR ($\theta_{śr}$ 83.0°)

Table 3. Results of the surface wettability test - OW method

Group no.	Contact angle, θ [°]				Surface free energy, (SFE) mJ/m^2	
	distilled water		diiodomethane			
Elektrochemically polished steel						
	Av.	SD	Av.	SD	Av.	SD
PE	**90.7**	1.0	**59.3**	0.3	**29.0**	0.2
PES	**78.3**	2.2	**52.8**	1.1	**33.4**	0.7
PESR	**73.2**	6.3	**59.3**	3.0	**33.0**	3.1
Nitrocarburized steel						
ANC	**113.5**	1.3	**63.5**	3.5	**29.3**	1.2
ANCS	**94.3**	4.9	**53.0**	1.7	**34.3**	1.5
ANCSR	**83.0**	4.8	**57.0**	2.4	**30.8**	1.6

3.4. Potentiodynamic study

The results of potentiodynamic tests of pitting corrosion resistance together with macroscopic evaluation of the surface were presented in Table 4 and Figs. 14-17. A beneficial effect of the produced layer on the parameters defining pitting corrosion resistance was observed. It was found that for such a modification method, for samples in the initial state, the values of: corrosion potential and breakdown potential and polarization resistance are higher than for polished samples. It was also observed that in the case of polished samples, sterilization and exposure to Ringer's solution increased corrosion resistance, in contrast to samples with a layer, where a decrease in the values of these parameters was observed. The obtained results confirm the macroscopic observations of the surfaces of the tested samples, indicating the initiation of corrosion pits - Fig. 15, 17.

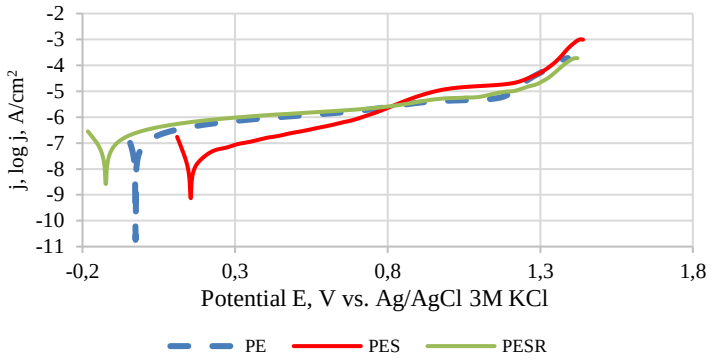

Fig. 14. Polarization curves for the electrochemically polished samples

Table 4. Results of potentiodynamic study

	E_{corr}, V		E_b, V		R_p, kΩ·cm²	
	Av.	SD	Av.	SD	Av.	SD
PE	**-0.044**	0.21	**+1.263**	0.26	**187**	0.65
PES	**+0.125**	0.42	**+1.364**	0.18	**395**	0.64
PESR	**-0.085**	0.35	**+1.357**	0.28	**203**	0.52
ANC	**+0.231**	0.33	**+1.408**	0.7	**321**	0.74
ANCS	**+0.102**	0.21	**+1.362**	0.6	**343**	0.68
ANCSR	**-0.097**	0.24	**+1.125**	0.32	**94**	0.22

Av. – average, SD – standard deviation

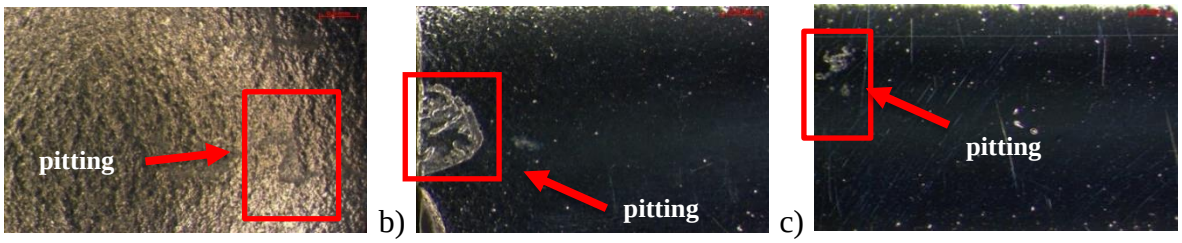

Fig. 15. Examples of corrosion damage on the samples surfaces: **a**) PE, **b**) PES, **c**) PESR, mag. 18.9 x

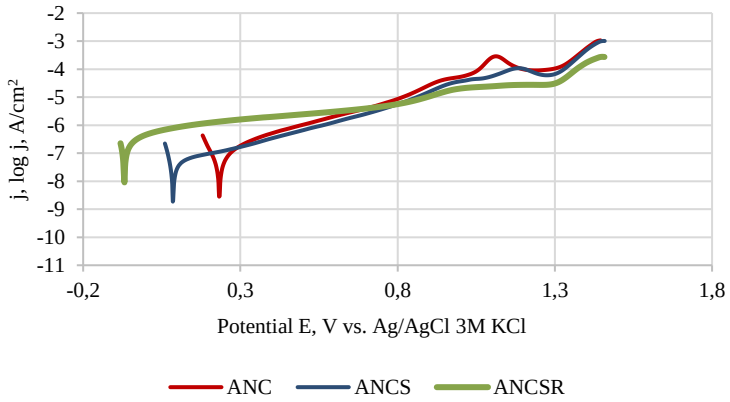

Fig. 16. Polarization curves for samples with the layer

Fig. 17. Examples of corrosion damage on the samples: **a**) PE, **b**) PES, **c**) PESR, mag. 18.9 x

3.5. Ions infiltration

The test results were presented in Table 5. It was found that the deposited nitrocarburized layer has influence on barrier properties. The presence of ions of the main alloying elements of the 316LVM steel such as Fe, Cr, Ni, Mo were found, but in smaller amounts for the samples with the deposited layer.

Table 5. Results of metallic ions infiltration

	Metallic ions infiltration tests, $\frac{\mu g}{cm^2}$ (mean value)							
	Fe	SD	**Cr**	SD	**Ni**	OS	**Mo**	SD
PE	**15.5**	0.65	**56.5**	1.10	**65.6**	1.42	**98.9**	2.01
PES	**7.5**	0.65	**49.9**	1.56	**59.8**	1.30	**97.9**	2.01

ANC	**9.9**	0.65	**50.1**	1.30	**58.8**	1.43	**92.8**	1.98
ANCS	**6.6**	0.63	**48.9**	1.30	**54.4**	1.38	**89.3**	1.80

The highest concentration of ions for all types of groups was recorded for Mo ions (98.9 $\frac{\mu g}{cm^2}$) whereas the lowest concentration was recorded for Fe ions (15.5 $\frac{\mu g}{cm^2}$). The highest barrier properties were observed for the layers on the samples subjected to sterilization and exposure to the Ringer's solution what from the point of view of the presence of the implant in a body is favorable. It can also be observed that the formation of the nitrocarburized layer resulted in a reduction in the mass of ions in the tested solution, in relation to polished samples. The greatest barrier was the layer for Fe ions.

3.6. Cytotoxicity studies

Based on the analysis of the colocalization of the color intensity of the fluorochrome cell survival was determined for all modifications in accordance with the applicable statistical principles (Fig. 18).

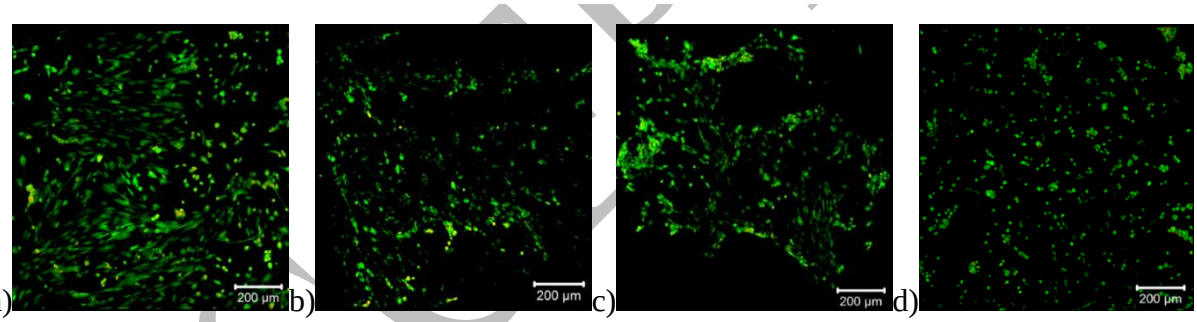

Fig. 18. Morphology and distribution of fibroblasts (PromoCell. DE), scanning confocal microscope: a) PE. b) PES. c) ANC, d) ANCS (green – live cells, red – necrotic cells)

In accordance with the requirements of ISO 10993: "A reduction in cell viability by more than 30% is considered a cytotoxic effect". Based on the obtained results, cell survival was found to be above 70% for all analyzed surface variants (Figs. 19 and 20).

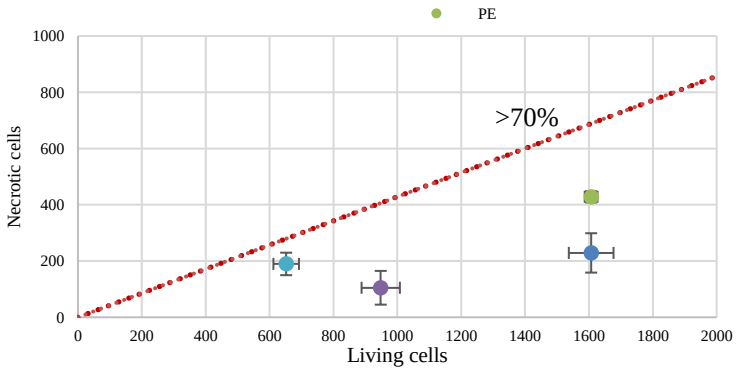

Fig. 19. Correlation between the number of necrotic cells and metabolically active cells

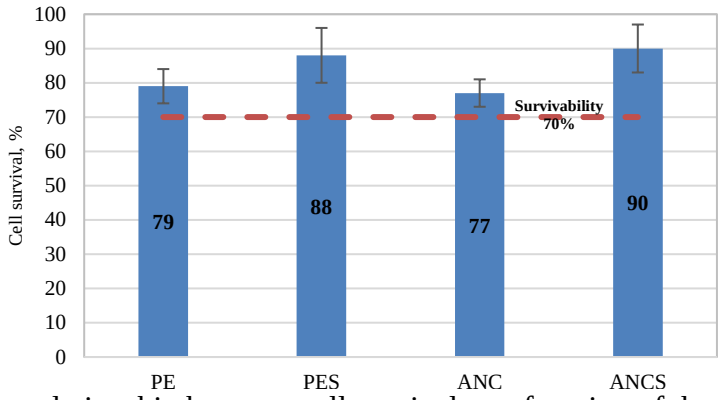

Fig. 20. The relationship between cell survival as a function of the analyzed area

The results of the lactate dehydrogenase level tests are presented in Fig. 21.

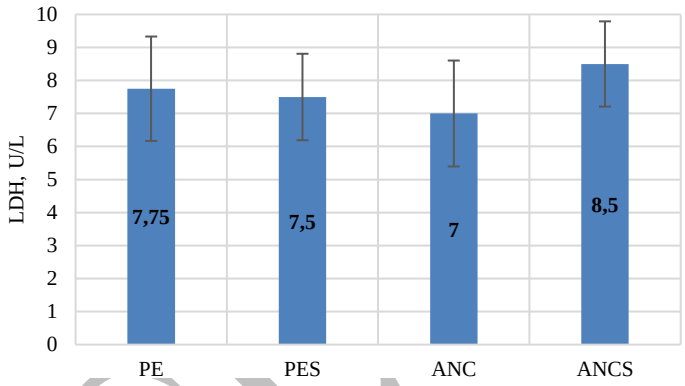

Fig. 21. Direct cytotoxicity based on the level of lactate dehydrogenase

5. Conclusion

The use of multi-element stabilizers for the surgical treatment of anterior chest wall deformities provides a very good final effect related to obtaining the correct chest curvature.

Previous studies, in most cases, were conducted on 316L steel [13,14,25]. 316LVM steel, compared to 316L, is characterized by a higher yield strength and tensile strength, which is associated with a higher percentage of Cr, Mo and Ni and a lower percentage of C, Cu, Si, P and S. Therefore, studies were conducted on samples with a layer prepared from a plate for the treatment of chest deformations. Based on the TEM results, it was found that both the substrate biomaterial and the layer crystallize in a cubic plane-centered lattice characteristic of the austenitic structure - Fig. 4. The TEM BF image clearly showed nitrided and carburized zones, separated by a separation boundary from the substrate. On this basis, it can be stated that the thickness of the surface layer produced at a temperature of 420°C was about 1.5 μm. This allowed for eliminating the participation of unfavorable elements in the layer, such as Cr and Ni. Based on the literature analysis, it can be concluded that the process temperature affects the

layer thickness, which is confirmed by the results of the authors [17] who produced layers at temperatures of 425°C and 475°C. They observed, that increasing the heat temperature significantly increases thickness. 425°C - 5 %CH_4 sample produced the smallest S-phase layer thickness with 3.47 ± 0.21 μm and followed by 425°C - 10 %CH_4 samples with 4.90 ± 0.25 μm and of 475°C - 5 %CH4 sample to 475°C - 10 %CH4 sample to 13.32 ± 0.48 μm. This is because higher temperature increases diffusion rate, increasing the thickness [22]. This is not beneficial due to the prebending of implants before they are introduced into the body. Thick layers are subject to cracking, which affects the unfavorable changes in the physicochemical properties of the surface.

The presence of the carbon-nitrogen layer was also confirmed by qualitative analysis of the chemical composition EDS. Both in the initial state, after sterilization and exposure, a gradient of C and N occurrence was shown, i.e. decreasing concentration of these elements with distance from the surface, which is characteristic of the occurrence of the carbon-nitrogen layer – Fig. 5. For polished samples, as well as with the layer, diffraction lines originating from the substrate from gamma iron Fe_γ (ICSD:98-005-3803) were identified, and additionally for the layer, diffraction lines originating from the Fe_4N_1 phase (ICSD:98-005-3503). In the studies, the phase detection threshold was about 3%, which made it difficult to identify the phase containing carbon.

A very important issue related to short-term implants is also the reactions that occur between their surface and the tissue environment. Implants of this type remain in the body for up to two years, therefore, in order to allow their removal, osteointegration should not occur on the surface. In this case, the physical properties of the surface play a very important role, which include: topography, wettability and free surface energy. Based on the analysis carried out using a scanning electron microscope (SEM), it was found that the surface of polished samples has an austenitic structure with visible slip bands and annealing twins (Fig. 7), while on the surface of samples with a layer - carbon-nitrogen austenite (Fig. 8). This confirms the previously obtained TEM results. In this case, no effect of sterilization or exposure was found on the structure of samples without a layer and with a layer. The surface topography analysis showed that microcracks occur on the deformed samples with a layer after sterilization and exposure (Fig. 9), but as proven in other studies, they did not significantly reduce the resistance to pitting corrosion. On the other hand, based on the results obtained using AFM atomic force microscopy, it was found that the formation of a layer did not significantly increase the Sa parameter in relation to the polished surface, the value of the Sa=25nm for PE samples and 29

nm for ANC samples. However, an increase in surface roughness was observed after sterilization and exposure - Table 2. The increase in roughness had an effect on wettability and surface energy.

Analyzing the results, a similar relationship can be observed, because the formation of the layer resulted in obtaining higher values of wetting angles – Table 3. For PE samples - θ_{av}=90.7°, while for ANCSR samples - θ_{av}=90.7°. The change of the surface character from hydrophobic to hydrophilic was influenced by sterilization and exposure to Ringer's solution. On the other hand, for polished samples, both sterilization and exposure influenced the obtaining of a hydrophilic surface (θ_{av}=78.3°, θ_{av}=73.2°, respectively). No significant differences were observed in the values of surface free energy. However, it can be stated that the type of surface polishing affects its wettability. Compared to an electrochemically polished surface, a mechanically polished surface is characterized by greater wettability (θ_{av}=83.2°) [35]. However, for electrochemically polished samples with a TiO2 coating produced by the ALD method, an increase in the contact angle value above 100 was observed [4]. Taking into account the environment in which the implant is located during stabilization, it can be stated that another important criterion for the suitability of the produced layer is its resistance to pitting corrosion. The test results showed an increase in corrosion resistance for samples with the produced layer – Table 4. In particular, it was found, respectively, for polished surfaces: E_{corr}=-0.044V, E_b=1.263V and R_p=187kΩ·cm^2, while for the layer: E_{corr}=+0.231V, E_b=1.408V and R_p =321kΩ·cm^2. For samples after sterilization, the values of the analyzed parameters are comparable, while sterilization and exposure resulted in a slight decrease in the analyzed parameters (E_{corr}=-0.097V, E_b =1.125V and R_p = 94kΩ·cm^2). The studies conducted by the authors of the publication [17] on 316 steel with nitrided and carburized layers confirm the increase in corrosion resistance and in particular in corrosion potential in relation to the substrate biomaterial. They also observed smaller pitting for samples with a layer.

Confirmation of obtaining favorable values of parameters characterizing corrosion resistance is the amount of metal ions released into the solution. The proposed surface modification resulted in the formation of a barrier layer against the release of the main alloying elements, such as: Cr, Ni, Mo and Fe. Additionally, sterilization of both polished samples and those with a layer reduced the mass density of metallic element ions in the solution - Table 5.

The most important issues concerning biomaterials and implants include the interaction of their surface with the surrounding cells. Therefore, as part of the biological assessment, cytotoxicity and cell viability tests were conducted using the direct method. Based on the

obtained results, cell survival was found to be above 70% for all analyzed surface variants, which indicates the lack of their cytotoxic effect; in particular for the sample: ANC - 77%, PE - 79%, PES - 88% and ANCS - 90% (Fig. 17,18,19). It can therefore be stated that sterilization had a positive effect on increasing cell survival. Also, based on the measurement of lactate dehydrogenase LDH, no significant differences in its level were found, therefore it can be stated that surface modification did not affect its cytotoxicity - Fig. 20.

In summary, it can be stated that the creation of a diffusion carbon-nitrogen layer has a beneficial effect on the physical and chemical properties of the implant surface and biocompatibility. Taking into account the obtained results, in the next stages the research methodology should be expanded to include fatigue tests of the layer, testing of the layer to assess the adhesion of S. aureus and E. coli bacterial colonies, and clinical studies.

In summary, the creation of a diffusion nitrocarburized layer had a positive effect on increasing hardness and abrasion resistance. This is of great importance for medical products, in which friction occurs between structural elements during operation. On the other hand, increasing biocompatibility is very important for implants used in the human body.

Taking into account the obtained results, in the next stages it is necessary to expand the research methodology in order to solve the following issues:

- fatigue tests of the layer in order to determine the possible decohesion process during cyclic loading,
- tests of the layer in order to assess the adhesion of S. aureus and E. coli bacterial colonies,
- conducting detailed biological tests taking into account irritation, sensitization and genotoxicity,
- for implants with a created layer, conducting tests in clinical conditions.

Biobliography

1. Aneja S., Taylor J.S., Soldes O., Dermatitis in patients undergoing the Nuss procedurefor correction of pectus excavatum, Contact Dermatitis, 2011, 65, DOI:10.1111/j.1600-0536.2011.01966.x.
2. Baranowska J., Arnold B., Corrosion resistance of nitrided layers on austenitic steel, Surf. Coat. Technol., 2006, (200)22-23, DOI:10.1016/j.surfcoat.2005.11.099.
3. Basiaga M., Jendruś R., Walke W., Paszenda Z., Kaczmarek M., Popczyk M., Influence of surface modification on properties of stainless steel used for implants, Arch. Metall. Mater., 2015, 60 DOI:10.1515/AMM-2015-0473.

4. Basiaga M., Walke W., Staszuk M., Kajzer W., Kajzer A., Nowińska K., Influence of ALD process parameters on the physical and chemical properties of the surface of vascular stents, Arch. Civ. Mech. Eng., 2017, 17 https://doi.org/10.1016/j.acme.2016.08.001
5. Borowski T., Adamczyk-Cieślak B., Brojanowska A., Kulikowski K., Wierzchoń T., Surface modification of austenitic steel by various glow-discharge nitriding methods, Mater. Sci., 2015, 21(3), DOI: 10.5755/J01.MS.21.3.7404.
6. Byrski A., Kopernik M., Major Ł., Kasperkiewicz K., Dyner M., Lackner J.M., Lumenta D., R Major, Characterization of biomaterials with reference to biocompatibility dedicated for patient-specific finger implants, Acta Bioeng Biomech, 2023, 25(1), DOI: 10.37190/ABB-02156-2022-02.
7. Casamassima M.G.S., Goldstein S.D., Salazar J.H., McIltrot K.H., Abdullah F., Colombani P.M., Perioperative strategies and technical modifications to the Nuss repair for pectus excavatum in pediatric patients: A large volume, single institution experience, J. Pediatr. Surg, 2014, 49(4), DOI:10.1016/j.jpedsurg.2013.11.058.
8. Cheng Z., Li C.X., Dong H., Bell T., Low temperature plasma nitrocarburising of AISI 316 austenitic stainless steel, Surf. Coat. Technol., 2005, (191)2-3, DOI:10.1016/j.surfcoat.2004.03.004.
9. de Sousa R.R.M., de Araújo F.O., Gontijo L.C., da Costa J.A.P., Alves C.Jr., Cathodic cage plasma nitriding (CCPN) of austenitic stainless steel (AISI 316): Influence of the different ratios of the (N2/H2) on the nitrided layers properties, Vacuum, 2012, (17)2, DOI:10.1590/S1516-14392013005000197.
10. Goldsztajn K., Godzierz M., Hercog A., Władowski M., Jaworska J., Jelonek K., Woźniak W.Kajzer A., Orłowska A., Szewczenko J.,Properties of biodegradable polymer coatings with hydroxyapatite on a titanium alloy substrate, Acta Bioeng Biomech, 2024, 26(1), DOI: 10.37190/ABB-02351-2023-03.
11. Górecki A., Babiak I., Leczenie zakażeń w obrębie narządu ruchu. Antybiotyki w profilaktyce i leczeniu zakażeń, Wydawnictwo Lekarskie PZWL, 2001.
12. Gregory D., Michael J., Goretsky T., Maripaz M., Kelly R.E.Jr, Nuss D., When it is not an infection: metal allergy after the Nuss procedure for repair of pectus excavatum, J. Pediatr. Surg., 2007, 42(1), DOI:10.1016/j.jpedsurg.2006.09.056.
13. Haïdopoulos M,, Turgeon S,, Sarra-Bournet C,, Laroche G,, Mantovani D., Development of an optimized electrochemical process for subsequent coating of 316 stainless steel for stent applications, J. Mater. Sci. Mater. Med., 2006, 17, DOI:10.1007/s10856-006-9228-4.

14. Hryniewicz T., Rokicki R., Rokosz K., Surface characterization of AISI 316L biomaterials obtained by electropolishing in a magnetic field, Surf. Coat. Technol., 2008, (202)9, DOI:10.1016/j.surfcoat.2007.07.067.
15. ISO 10993-5 - Biological evaluation of medical devices, Part 5: Tests for in vitro cytotoxicity.
16. ISO 5832-1: Implants for surgery - Metallic materials - Part 1: Wrought stainless steel.
17. Juri Afifah Z., Azmi F., Basak A., Ghani J., Kasim M.S., Alias R., Tribological and corrosion behaviour of medical grade 316LVM steel by low temperature hybrid gaseous nitriding and carburizing, Tribol. Int., 2023, 190, DOI:10.1016/j.triboint.2023.109026.
18. Kajzer A., Kajzer W., Dzielicki J., Matejczyk D., The study of physicochemical properties of stabilizing plates removed from the body after treatment of pectus excavatum, Acta Bioeng Biomech, 2015, 2, DOI:10.5277/ABB-00140-2014-02.
19. Kajzer A., Rabij K., Basiaga M., Nowińska K., Kaczmarek M., Borowski T., Wierzchoń T., Influence of sterilization and exposure to the Ringer's solution on mechanical and physicochemical properties of nitrocarburized 316 LVM steel, Arch. Metall. Mater., 2018, (63)3, DOI:10.24425/123799.
20. Kajzer W., Kajzer A., Grygiel-Pradelok M., Ziębowicz A., Ziębowicz B., Evaluation of physicochemical properties of TiO_2 layer on AISI 316 LVM stainless steel intented for urology. Springer International Publishing, 2016, DOI:10.1007/978-3-319-39904-1_34.
21. Kelly R.E., Goretsky M.J., Obermeyer R., Kuhn M.A., Redlinger R., Haney T.S., Moskowitz A., Nuss D, Twenty-one years of experience with minimally invasive repair of pectus excavatum by the Nuss procedure in 1215 patients, Ann Surg, 2010,163(3), DOI:10.1016/j.jtcvs.2020.11.154.
22. Li X.Y., Thaiwatthana S., Dong H., Bell T., Thermal stability of carbon S phase in 316 stainless steel. Surf. Eng., 2002, 18, DOI:10.1179/0267084022250062.
23. Liu Y., Zhu D., Jeremy D.P., Gilbert L., Fretting Initiated Crevice Corrosion of 316LVM Stainless Steel in Physiological Phosphate Buffered Saline, Acta Biomater., 2019, (97)1, DOI:10.1016/j.actbio.2019.07.051.
24. Martínez O.L., Pérez F.J., Gómez C., The effect of nitrogen ion implantation on the corrosion behaviour of stainless steels in chloride media, Surf. Coat. Technol., 2005, (200)5-6, DOI:10.1016/j.surfcoat.2005.08.034.
25. Niua W., Lillarda R.S., Lib Z., Ernst F., Properties of the Passive Film Formed on Interstitially Hardened AISI 316L Stainless Steel, Electrochim. Acta., 2015, 176(4):410-419.

26. Orłowska A., Szewczenko J., Kajzer W., Goldsztajn K., Basiaga M., Study of the effect of anodic oxidation on the corrosion properties of the Ti6Al4V implant produced from SLM, J. Funct. Biomater., 2023, 14(4), DOI:10.3390/jfb14040191.
27. Park H.J., Lee S.Y., Lee C.S., Complications associated with the Nuss procedure: analysis of risk factors and suggested measures for prevention of complications, J. Pediatr. Surg., 2004, 39(3), DOI:10.1016/j.jpedsurg.2003.11.012.
28. PN-EN ISO 10993-15 Biological evaluation of medical devices — Part 15: Identification and quantification of degradation products from metals and alloys.
29. Pokrowiecki R., Tyski S., Zaleska M., Problematyka zakażeń okołowszczepowych, Post. Mikrobiol., 2014, 53(2):123-134.
30. Rosato E., Giovannetti A., Rossi C., Menghi G., Pisarri S., Salsano F., Recurrentinfections in patients with nickel allergic hypersensitivity, J. Biol. Regul. Homeost Agents, 2009, 23(3):173-180.
31. Schalock P.C., Menné T., Johansen J.D., Hypersensitivity reactions to metallic implants − diagnostic algorithm and suggested patch test series for clinical use, Contact Dermatitis, 2011, 66, DOI:10.1111/j.1600-0536.2011.01971.x.
32. Shah B., Cohee A., Deyerle A., Kelly C.S., Frantz F., Kelly R.E., Kuhn M.A., Lombardo M., Obermeyer R., Goretsky M.J., High rates of metal allergy amongst Nuss procedure patients dictate broader pre-operative testing, J. Pediatr. Surg., 2014, (49)3, DOI:10.1016/j.jpedsurg.2013.07.014.
33. Shen L., Wang L., Xu J.J., Plasma nitriding of AISI 304 austenitic stainless steel assisted with hollow cathode effect, Surf. Coat. Technol., 2013, (204)20, DOI:10.1016/j.surfcoat.2010.03.018.
34. Shin S., Goretsky M.J., Kelly R.E. Jr, Gustin T., Nuss D., Infectious complications after the Nuss repair in a series of 863 patients, Pediatr. Surg., 2007, 42(1), DOI:10.1016/j.jpedsurg.2006.09.057.
35. Wanga X., Zhaoa L., Dinga M.H, Zhenga H., Zhanga H.S., Zhanga B., Lia X.Q., Wua G.Y., Surface modification of biomedical AISI 316L stainless steel withzirconium carbonitride coatings, Appl. Surf. Sci., 2015, 340, http://dx.doi.org/10.1016/j.apsusc.2015.02.191.
36. Welch K.J., Satisfactory surgical correction of pectus excavatum deformity in childhood, J. Thorac. Surg., 1958, 36:697-713.
37. Wielowiejska G.A., Wiśniewski T., Rubach R., Fretting corrosion studies of materials used for elements of hip joint endoprostheses, Tribologia, 2018, 5:143-151.

38. Wu P.C., Knauer E.M., McGowan G.E., Hight D.W., Repair of pectus excavatum deformities in children: a new perspective of treatment using minimal access surgical technique, Arch. Surg., 2016, 136(4):419-424.
39. Ziębowicz A., Sambok-Kiełbowicz A., Walke W., Mzyk A., Kosiel K., Kubacki J., Bączkowski B., Pawlyta M., Ziębowicz B., Evaluation of Bacterial Adhesion to the ZrO_2 Atomic Layer Deposited on the Surface of Cobalt-Chromium Dental Alloy Produced by DMLS Method, Materials, 2021, 14(5), DOI:10.3390/ma14051079.